*AMSE JOURNALS-AMSE IIETA publication-2017-Series: Modelling A; Vol. 90; N°3; pp 296-309*
*Submitted Sept. 18, 2017; Revised Jan. 04, 2018; Accepted Jan. 08, 2018*

# Contactless Measurement of Voltage Harmonics on Low Voltage Multi-conductor Cables

*César D. P. Crovato, **Cristian F. Santos, ***Tiago A. Pereira, ****Roberto C. Leborgne, *****Valner J. Brusamarello

* Programa de Pós-Graduação em Engenharia Elétrica, Unisinos University, São Leopoldo, BRAZIL (e-mail: ccrovato@unisinos.br, cesarcrovato@gmail.com).
**Programa de Pós-Graduação em Engenharia Elétrica, (Master Program) Unisinos University, São Leopoldo, BRAZIL (e-mail: fsantoscristian@gmail.com).
***Programa de Pós-Graduação em Engenharia Elétrica, (Master Program) Unisinos University, São Leopoldo, BRAZIL (e-mail: tiagoanacleto@gmail.com).
****Roberto C. Leborgne is with Federal University of Rio Grande do Sul, Porto Alegre, Brazil (e-mail roberto.leborgne@ufrgs.br).
*****Valner J. Brusamarello Leborgne is with Federal University of Rio Grande do Sul, Porto Alegre, Brazil (e-mail brusamarello.valner@gmail.com)

## Abstract

This paper presents a feasibility study on measure voltage harmonics with a contactless device, on multi-conductor cables. The demonstration is given by a four-conductor cable with a variety of standard dimensions, using an external calibration signal, given the capability to adjust itself "on field". The results show the proposed methodology is suitable to be used in an electronic circuit; even with many random sources of error, simulated in the environment test.

## Key words

Contactless voltage measurement, Harmonic voltage measurement, Power quality, Harmonic distortion.

## 1. Introduction

Recent search efforts in non-intrusive voltage and current waveform measurement are mainly focused in monitoring energy consumption and power factor (at fundamental frequency) determination[1][2]. Also, there still difficulties in high accuracy measurements of harmonics and scaling factor of voltage waveform [3][4].

The voltage and current in a conductor may be determined by electric and magnetic field sensors placed nearby. In this technique, the measurement of voltage and current from a conductor can be performed without removing the insulation. Non-contact sensors have low cost of installation because they do not require the shutdown of power [3].

Non-contact electromagnetic field sensors can monitor voltage and current in multiple-conductor cables from a distance. Knowledge of the cable and sensor geometry is generally required to determine the transformation that recovers voltages and currents from the sensed electromagnetic fields [3][5].

In [3] the authors present a calibration technique that enables the use of non-contact sensors without the prior knowledge of conductor's geometry. Calibration of the sensors is accomplished with a reference load or through observation of in situ loads, obtaining a maximum difference of 1% over a dynamic range of 1000W, when comparing with commercial measurement equipment, both installed on the feeder cable of a three-phase 208/120V laboratory electrical service. However, the assumption of at least three-phase voltage symmetry is still necessary. Also, the "implicit" calibration, without the "reference load" can add error reported around 2%. The linearity voltage sensing is better than ±5% up to 300V and 300Hz [4]. Also, the sensor must be calibrated against a known reference voltage in applications needing high accurate voltage measurement, otherwise there will be an error in the waveform, by a constant and unknown factor; nevertheless, the authors argue that many power quality metrics—such as total harmonic distortion—are unaffected by changes of a constant.

In [1], the authors present a new non-intrusive AC voltage measurement technique based on stray electric field energy harvesting. Autonomous switches are used to monitor the stored electric field energy in a storage capacitor and to generate pulse train. Experimental results show that the repetition rate of the output pulse is a linear function of the line voltage. The research is at an initial and has not mentioned possible interferences and reliable calibration procedures, also, is focused only at fundamental frequency.

In [6], the authors present a non-invasive approach for measuring low-voltage (230−400V) waveform using cylindrical capacitor coupled directly in each cylindrical conductive element. They also present a conditioning circuit less susceptive to geometry of wires from 1.5 $mm^2$ to 16

$mm^2$ of cross section area. The comparison between the proposed non-intrusive method and a direct measurement of the voltage shows high accuracy with a maximum error lower than 1%. Also, do not require any *in situ* calibration, in a controlled environment.

A complete voltage measurement system with uncertainty below 2% are presented in [7]. Also, a three-phase version of [4] with uncertainties up to 3% on voltage measurement is presented in [8]. It is important to notice that the plastic case used in [8] configure a pre-determined and regular geometry for the separation of wires. This plastic case establishes fixed couple capacitances passible to create crosstalking and reducing the overall accuracy. Also, the very low capacitance on multi-conductor cable wires will require very high front end resistance as shown in [3], thus this topology is suitable only for single cable, but in most industrial feeder multi-conductor cable is very common.

A two-sensor head capacitive probe has been successfully implemented for non-contact single phase AC voltage measurement. The system is able to extract the relationship between the induced currents and the supply voltage and presents a fitted model with estimated uncertainty around 5% for fundamental frequency [2].

A non-contact voltage sensor for transmission lines, based on differential voltage measurement is presented in [9]. The system is in self-integration mode circuit over a suspended common mode voltage, making this a non-grounded sensor. An array of several sensors is simultaneously used in order to maintain the uniformity of electric field distribution and reduce the distortion caused by the sensors themselves. The reported uncertainty is below 0.5%.

The electric-field state is detected using Field Effect Transistor (FET) as sensor of electric-field based on the capacitance effect principle [10]. Then the charged state of conductor should be indirectly detected by electric-field state. In [11] a large (25 cm) and fixed cylindrical sensor with 2 electrodes is used to clamp a single wire with unknown voltage. The RMS voltage on the wire can be determined by injecting a known voltage waveform through the structure and performing the measurements on a digital processor on the frequency [11] or time [12] domain. The reported uncertainties were less than 0.75% from 60Hz to 1000Hz range, with 7 different relative wire positions in the sensor.

Other devices and techniques are reported to be applied in contactless voltage measurement such as MEMS and resonators, among others [13]-[20].

In this article, we present a contactless sensor conception of a small form factor to be applied in low voltage measurements on multiple-conductor cables, independent of geometry, capable to be calibrated in situ. The presented sensor has relatively low complexity, no voltage symmetry constraints and also power quality standard compliant. Table 1 presents the summary review of

sensors presented in this section with the main characteristics.

Tab. 1 Some Research Overview on Non-Contact Voltage Measurement

| *Paper* | *A* | *B* | *C* | *D* |
|---|---|---|---|---|
| [3] | X | - | X | X |
| [4] | X | - | X | X |
| [1] | - | X | - | X |
| [6] | X | X | - | X |
| [7] | X | X | - | X |
| [8] | X | X | - | X |
| [2] | X | X | - | X |
| [9] | - | X | - | - |
| [10] | X | X | - | X |
| [11] | X | X | - | X |
| [11] | X | X | - | X |

A: small form factor

B: no assumption about voltage magnitude and/or phase

C: multi-conductor cable voltage measurement (feeder cable "as is").

D: relative low complexity and low cost.

## 2. The Proposed Hardware and Methodology

### 2.1 Modeling

Figure 1 shows the perspective (a) and transversal (b) view of the proposed hardware; it consists in a metallic hollow cylinder, connected to the reference (*gnd*) of the conditioning electronic circuit. This cylinder has an aperture and a join (omitted in the figure) to clamp a multi-conductor cable (c). Internally, there are several (*N*) multiplexed plates around the circumference of the cylinder (*N=16* on Figure 1b), creating, by symmetry, the same capacitance C from each plate to the reference *gnd* (d). In parallel with C, there is the conditioning electronic circuit, with details omitted in Figure1 by simplicity, except for the input resistance R. Also, in Figure 1c, the multi-conductor cable has four wires, with the voltages $v_1$, $v_2$, $v_3$, $v_4$ that can be $v_{ag}$ or $v_{bg}$ or $v_{cg}$ or $v_{ng}$ (voltages from phases *a*, *b*, *c* and *neutral*, to the ground), in any random order. Therefore, from the wires to each single "*i*" plate around circumference, there are coupling capacitances $c_{i1}$, $c_{i2}$, $c_{i3}$, $c_{i4}$ respectively. If the reference of the electronic conditioning circuit is connected to an available neutral, for example, on an outside outlet, the equivalent circuit can be summarized as in Figure 1e. and the voltages of wires becomes $v_{an}$, $v_{bn}$, $v_{cn}$ and $v_{nn}$. By definition

$v_4$=$v_{nn}$=*0*, and $v_1$, $v_2$, and $v_3$ are in anti-clockwise, so, this circuit has a sensing voltage at C (in according to Figure 1d model), called $s_i$, for *i*-st plate, in frequency domain:

$$\vec{s}_i = \frac{\left(c_{1i}\vec{v}_1 + c_{2i}\vec{v}_2 + c_{3i}\vec{v}_3\right) j\varpi}{\left(C + c_{1i} + c_{2i} + c_{3i} + c_{4i}\right) j\varpi + 1/R} \tag{1}$$

The arrow notation means a complex (or phasor) quantity specifically at frequency ω [rad/s]. Also, the impedance at the same point can be calculated:

$$\vec{z}_i = \left[\left(C + c_{1i} + c_{2i} + c_{3i} + c_{4i}\right) j\varpi + 1/R\right]^{-1} \tag{2}$$

Replacing (2) in (1):

$$\left(c_{1i}\vec{v}_1 + c_{2i}\vec{v}_2 + c_{3i}\vec{v}_3\right) = \frac{\vec{s}_i}{\vec{z}_i\, j\varpi} \tag{3}$$

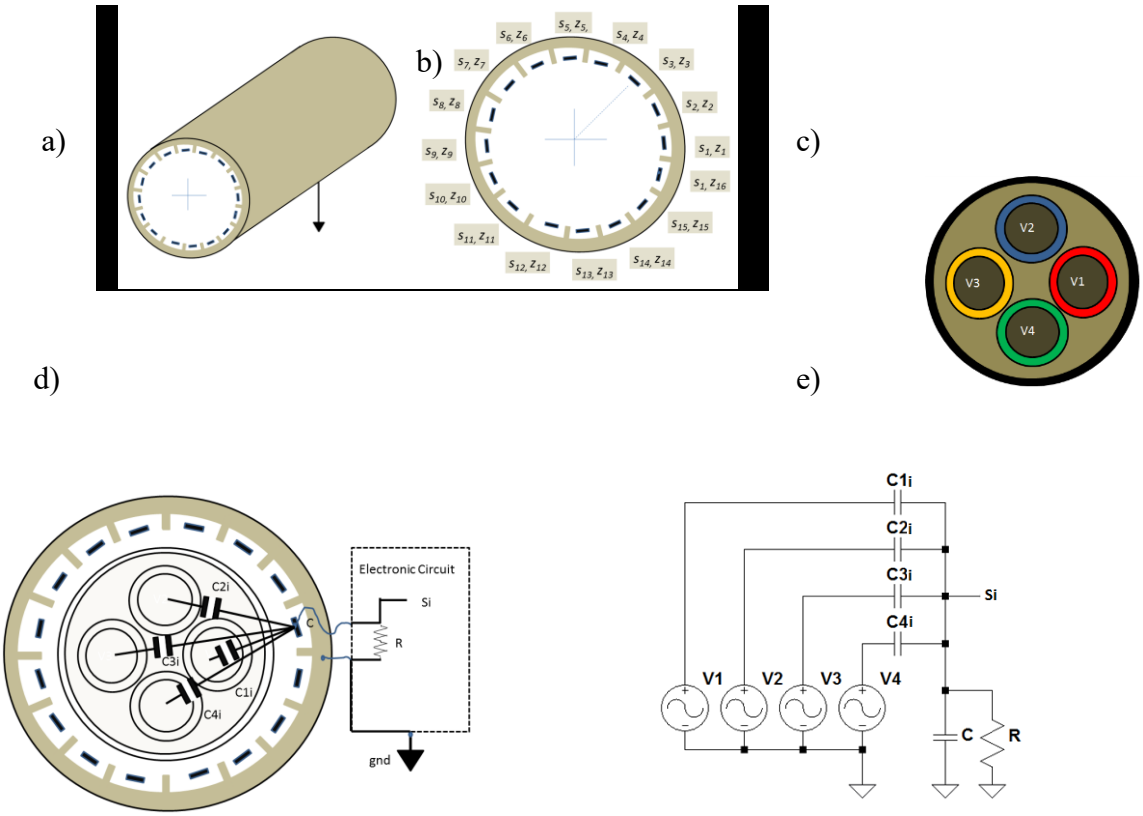


Fig. 1. Respectively: a) perspective view of the proposed hardware, b) transversal view, c) four wire multi-conductor cable, d) coupled capacitances and sensing system for an aleatory "i" plate around circumference, e) equivalent circuit.

The “electronic circuit” box in Figure 1c is able to inject a known current at known frequency in order to determine zi. As C and R, are also known, it is possible to determine:

$$c_{tot\_i} = c_{1i} + c_{2i} + c_{3i} + c_{4i} \tag{4}$$

If at frequency ωz there is only an unknown zero sequence voltage vz, (3) becomes:

$$\left(c_{1i} + c_{2i} + c_{3i}\right)\vec{v}_z = \frac{\vec{s}_i}{\vec{z}_i j\varpi}, \qquad \varpi = \varpi_z \tag{5}$$

Each of the four wires, in multi-conductor cable, contributes with ¼ of overall capacitance ctot_i. At average, each conductor contributes with ¼ of overall capacitance, considering all sensors around circumference, then (5) can be rewrite as:

$$\left(c_{tot\_i} - \frac{c_{tot\_i}}{4}\right)\vec{v}_z \cong \frac{\vec{s}_i}{\vec{z}_i j\varpi}, \qquad \varpi = \varpi_z \tag{6}$$

For many plate sensors around circumference (N≥128), from (6), voltage vz can be found using the pseudoinverse operation (A-1~ A+):

$$\vec{v}_z \cong \begin{bmatrix} c_{tot\_1} - c_{tot\_1}/4 \\ c_{tot\_2} - c_{tot\_2}/4 \\ \cdots \\ c_{tot\_N} - c_{tot\_N}/4 \end{bmatrix}^{+} \begin{bmatrix} \vec{s}_1/\left(\vec{z}_1 j\varpi\right) \\ \vec{s}_2/\left(\vec{z}_2 j\varpi\right) \\ \cdots \\ \vec{s}_N/\left(\vec{z}_N j\varpi\right) \end{bmatrix}, \qquad \varpi = \varpi_z \tag{7}$$

The next step is to find the sensors aligned with the geometrical quadrature of wires, as shown in Figure 2a, with vz still at frequency ωz.

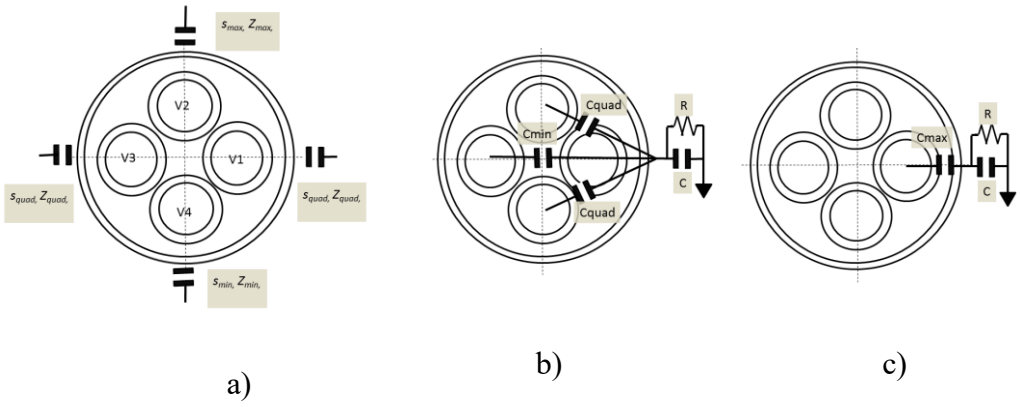


a) b) c)

Fig. 2. a) Sensors in quadrature with wires on four conductor cable, b) Capacitances cmin, cmax and cquad coupled with one of the quadrature sensor plate, c) Capacitances cmin, cmax and cquad coupled with one of the quadrature sensor plate.

The index of the sensor with the lowest voltage is “i=imin”, which should be the nearest to the neutral wire and the index of sensor with the highest voltage is “i=imax” which should be the farthest to the neutral wire. The quadrature sensors verify “i= iquad= imin ±(imax- imin)/2”. Considering the sensors with index imax, imin and iquad (here, the sensor at right), there are only three possible values for the coupling capacitances cmin, cmax and cquad. Hence, using (5) it is possible to create the relationship:

$$\begin{bmatrix} \vec{v}_z & 0 & 2\vec{v}_z \\ 0 & \vec{v}_z & 2\vec{v}_z \\ \vec{v}_z & \vec{v}_z & \vec{v}_z \end{bmatrix} \begin{bmatrix} c_{\max} \\ c_{\min} \\ c_{\text{quad}} \end{bmatrix} = \begin{bmatrix} \vec{S}_{i\max} /(\vec{z}_{i\max} j\varpi) \\ \vec{S}_{i\min} /(\vec{z}_{i\min} j\varpi) \\ \vec{S}_{i\text{quad}} /(\vec{z}_{i\text{quad}} j\varpi) \end{bmatrix}, \qquad \varpi = \varpi_z \tag{8}$$

and,

$$\begin{bmatrix} c_{\max} \\ c_{\min} \\ c_{\text{quad}} \end{bmatrix} = \begin{bmatrix} \vec{v}_z & 0 & 2\vec{v}_z \\ 0 & \vec{v}_z & 2\vec{v}_z \\ \vec{v}_z & \vec{v}_z & \vec{v}_z \end{bmatrix}^{+} \begin{bmatrix} \vec{S}_{i\max} /(\vec{z}_{i\max} j\varpi) \\ \vec{S}_{i\min} /(\vec{z}_{i\min} j\varpi) \\ \vec{S}_{i\text{quad}} /(\vec{z}_{i\text{quad}} j\varpi) \end{bmatrix}, \qquad \varpi = \varpi_z \tag{9}$$

Knowing the values of cmin, cmax and cquad it is possible to apply (3) to find any voltages on wires, using only the readings of sensors of index imax, imin and, iquad

$$\begin{bmatrix} c_{\text{quad}} & c_{\max} & c_{\text{quad}} \\ c_{\text{quad}} & c_{\min} & c_{\text{quad}} \\ c_{\max} & C_{\text{quad}} & c_{\min} \end{bmatrix} \begin{bmatrix} \vec{v}_1 \\ \vec{v}_2 \\ \vec{v}_3 \end{bmatrix} = \begin{bmatrix} \vec{S}_{i\max} /(\vec{z}_{i\max} j\varpi) \\ \vec{S}_{i\min} /(\vec{z}_{i\min} j\varpi) \\ \vec{S}_{i\text{quad}} /(\vec{z}_{i\text{quad}} j\varpi) \end{bmatrix} \tag{10}$$

for any frequency $\omega$. And,

$$\begin{bmatrix} \vec{v}_1 \\ \vec{v}_2 \\ \vec{v}_3 \end{bmatrix} = \begin{bmatrix} c_{\text{quad}} & c_{\max} & c_{\text{quad}} \\ c_{\text{quad}} & c_{\min} & c_{\text{quad}} \\ c_{\max} & C_{\text{quad}} & c_{\min} \end{bmatrix}^{+} \begin{bmatrix} \vec{S}_{i\max} /(\vec{z}_{i\max} j\varpi) \\ \vec{S}_{i\min} /(\vec{z}_{i\min} j\varpi) \\ \vec{S}_{i\text{quad}} /(\vec{z}_{i\text{quad}} j\varpi) \end{bmatrix} \tag{11}$$

An extra information is necessary to determine which voltage corresponds to phase *a*, *b* or *c* such as a pilot signal and a load for calibration purposes. This calibration load also needs drain

current with only zero sequence component at a certain frequency $\omega_z$, in order to create the voltage $v_z$ at the measurement point. The positive sequence at fundamental frequency, allows determining the sequence of phases.

Alternatively, it is possible to combine, in average sense, the results for several $v_z$, using the calibration load and other triplet harmonics that are usually zero sequence in industrial environment, to obtain the values of $c_{min}$, $c_{max}$ and $c_{quad}$ (9) and then $v_1$, $v_2$, and $v_3$ (11).

Alternatively, it is possible to combine the results for several $v_z$, using the calibration load and other triplet harmonics, that are usually zero sequence in industrial environment, to obtain the values of $c_{min}$, $c_{max}$ and $c_{quad}$ (9) and then $v_1$, $v_2$, and $v_3$ (11).

Figure 3 shows details of the electronic circuit connected to all plate sensors such as the multiplexing capability, impedance measurement capability (through the current source $Iz$) and sensing/amplifying capability. Because the $Z_i$ can be measured at any time, accurate components for $R$ and $C$ are not required.

In addition, the losses and dissipation factor of the dielectric of cables and plates are omitted in this study; however, its influence can be taken into consideration. Because the impedance is measured at any time, these values can be expressed as a function of capacitances, turning the equations a little more complex, but still solvable.

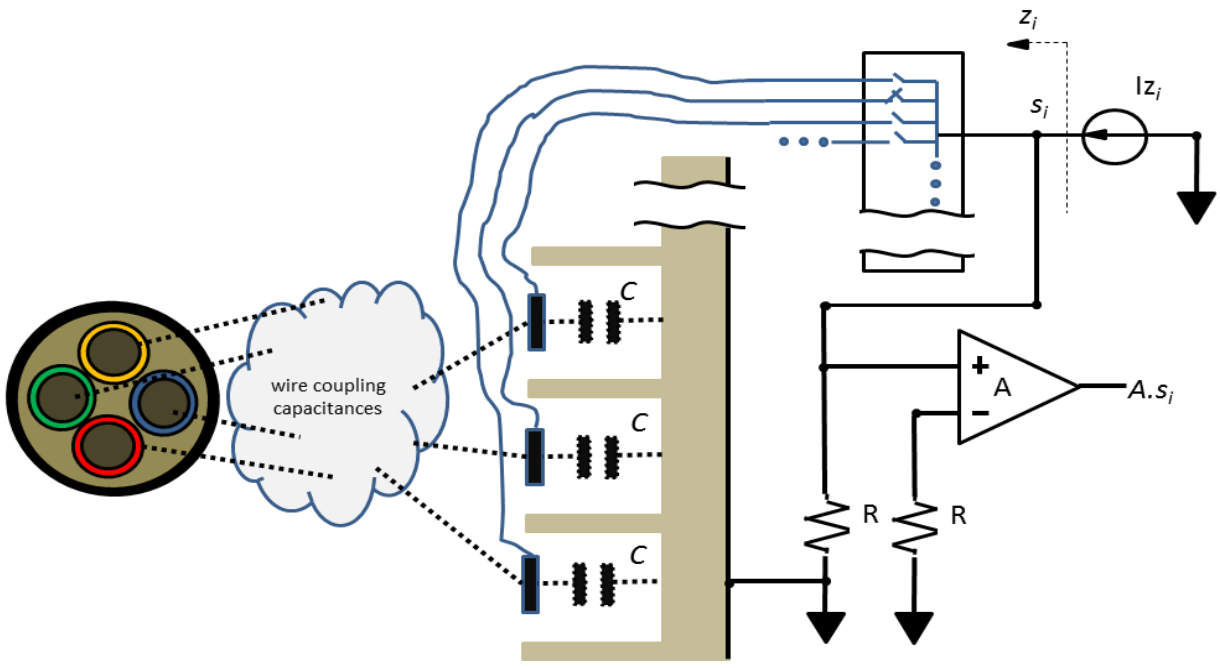


Fig. 3. Electronic Conditioning details of the proposed sensor

### 2.2 Cable capacitance simulation

Table 2 summarizes the typical geometry on four-conductor cables. Used for estimating the capacitance for several conductors and isolations' diameters and thickness.

Tab. 2 Typical dimensions on multi-conductor (4 wires) cables

| *Nominal Section [mm²]* | *External Diameter[ mm]* | *Conductor diameter [mm]* | *Isolation thickness [mm]* | *Cover thickness [mm]* |
|---|---|---|---|---|
| 4x1.5 | 9.5 | 1.5 | 0.7 | 1.0 |
| 4x2.5 | 10.6 | 1.9 | 0.7 | 1.1 |
| 4x4 | 11.6 | 2.5 | 0.7 | 1.1 |
| 4x6 | 13.2 | 3.1 | 0.7 | 1.2 |
| 4x10 | 15.7 | 4.1 | 0.7 | 1.2 |
| 4x16 | 19.9 | 5.1 | 0.7 | 1.3 |
| 4x25 | 24.7 | 6.5 | 0.9 | 1.4 |
| 4x35 | 27.8 | 7.3 | 0.9 | 1.5 |
| 4x50 | 32.3 | 9.0 | 1.0 | 1.6 |
| 4x70 | 37.5 | 10.4 | 1.1 | 1.8 |
| 4x95 | 41.8 | 12.0 | 1.1 | 1.9 |
| 4x120 | 46.9 | 14.0 | 1.2 | 2.0 |

### 2.3 Experimental Simulation Setup

The simulation was performed in MatLab and the generated signals contain a different set of modules and phases of harmonics which are combined resulting in a large set of test-cases.

The harmonics values for simulation are determined according to definitions from IEC 61000-4-30 [21],

IEC-61000-4-7 [22] and IEC 61000-2- 4 [23]. In [21] it is established for Class A equipment that they must be able to read voltages in harmonic domain accurately, according with methodology described in [22]. The measuring range must be from 10% to 200% for each one of the harmonics applied from "Class III environment" specified in [23], even on presence of influence quantity of 200% of one other harmonic also specified in "Class III environment" [23]. Table 3 summarizes this setup:

Tab 3. Boundaries for Measurement of '*k*' order Harmonic on Range: $200\%U_k \geq \widetilde{U}_k > 10\%U_k$

| **Conditions** | **Maximum uncertainty** $e_{MAX_K}$ | **Influence Quantity**[1] |
|---|---|---|
| $\widetilde{U}_k \geq 1\%U_{nom}$ | $\pm 5\%\widetilde{U}_k$ | $200\%U_p$ |
| $\widetilde{U}_k < 1\%U_{nom}$ | $\pm 0.05\%U_{nom}$ | $200\%U_p$ |

[1] with $p$ being any number, since: $(p \in \mathbf{N}) \cup (p > 1)$ except for $p = k$

$U_k$ and $U_p$ come from Table 4.

$U_{nom}$ is the nominal voltage of measurement equipment, also referred to as $U_{din}$. $\widetilde{U}_k$ is the "k" order harmonic value to be read, under $U_p$, the "p" order harmonic influence quantity. The "p" can be any other order from 2 to typically 50, except of course, p=k. $U_k$ is the maximum "k" order harmonic value (as % of fundamental component) allowable in industrial environments. The values for $U_k$ and $U_p$ can be extracted from Table 4, according to [23]. Therefore, as the "worst case" must be evaluated, the waveforms in (12) must be considered on each wire respectively.

Tab 4. Maximum ("x" order ) Individual Harmonic % value of Udin, recommended for industrial environment (Class III).

| ***x*** | ***$U_x$ [%]*** | ***x*** | ***$U_x$ [%]*** | ***x*** | ***$U_x$ [%]*** | ***x*** | ***$U_x$ [%]*** |
|---|---|---|---|---|---|---|---|
| 2 | 3.0 | 15 | 2.0 | 28 | 1 | 41 | 2.59 |
| 3 | 6.0 | 16 | 1.0 | 29 | 3.079 | 42 | 1 |
| 4 | 1.5 | 17 | 4.0 | 30 | 1 | 43 | 2.529 |
| 5 | 8.0 | 18 | 1.0 | 31 | 2.978 | 44 | 1 |
| 6 | 1.0 | 19 | 4.0 | 32 | 1 | 45 | 1 |
| 7 | 7.0 | 20 | 1.00 | 33 | 1 | 46 | 1 |
| 8 | 1.0 | 21 | 1.75 | 34 | 1 | 47 | 2.419 |
| 9 | 2.5 | 22 | 1.0 | 35 | 2.803 | 48 | 1 |
| 10 | 1.0 | 23 | 3.5 | 36 | 1 | 49 | 2.369 |
| 11 | 5.0 | 24 | 1.0 | 37 | 2.726 | 50 | 1 |
| 12 | 1.0 | 25 | 3.5 | 38 | 1 | | |

| | | | | | |
|---|---|---|---|---|---|
| 13 | 4.5 | 26 | 1 | 39 | 1 |
| 14 | 1.0 | 27 | 1 | 40 | 1 |

[x] means the harmonic order, so *x* could be *p* or *k*

$$\begin{aligned} u_{kpA}(t) &= \sqrt{2}\mathrm{U}_{\mathrm{din}}\cos(2\pi f_0 t) + \sqrt{2}\widetilde{\mathrm{U}}_{\mathrm{k}}\cos(2\pi k f_0 t) + 2\sqrt{2}\mathrm{U}_{\mathrm{p}}\cos(2\pi p f_0 t), \\ u_{kpB}(t) &= \sqrt{2}\mathrm{U}_{\mathrm{din}}\cos(2\pi f_0 t + 240\pi/180) + \sqrt{2}\widetilde{\mathrm{U}}_{k}\cos(2\pi k f_0 t + k240\pi/180) + 2\sqrt{2}\mathrm{U}_{\mathrm{p}}\cos(2\pi p f_0 t + p240\pi/180) \\ u_{kpC}(t) &= \sqrt{2}\mathrm{U}_{\mathrm{din}}\cos(2\pi f_0 t + k120\pi/180) + \sqrt{2}\widetilde{\mathrm{U}}_{\mathrm{k}}\cos(2\pi k f_0 t + k120\pi/180) + 2\sqrt{2}\mathrm{U}_{\mathrm{p}}\cos(2\pi p f_0 t + k120\pi/180), \quad f_0 = 60Hz \end{aligned} \tag{12}$$

Thus, in order to determine the suitability of an amplification stage (as depicted in Figure 3), the differential and common mode voltage will be evaluated under the waveforms defined by (12), for $\widetilde{U}_k$=200%$U_k$ and $\widetilde{U}_k$=10%$U_k$ for all possible influence quantities using the [21] and [23] criteria, with R=2MΩ, C=10pF.

These values for R and C are chosen in order to maintain appropriate noise to signal relation, excursion of signal and condition to determine the capacitances of wires.

Also, thousands of different scenarios were simulated for each type of cable in Table 2. For each scenario it was measured the normalized error on harmonic "k", defined as follows:

$$e_{Nk} = \frac{\left|\widetilde{U}_k - \widetilde{\widetilde{U}}_k\right|}{e_{MAX_K}}[pu] \tag{13}$$

Where $e_{MAX_K}$ is the maximum allowable error (from conditions defined on Table 2I), $\widetilde{U}_k$ is the value to be read and $\widetilde{\widetilde{U}}_k$ is the actual reading value. If $e_{Nk}$ reaches above 1pu at least in 0.1% of all test cases, it will be considered a non-compliant system.

Three sources of errors were inserter in order to test the system: a) errors of misalignments between the cables and the sensor quadrature until 1.4 degrees; b) pilot signal, with positive and negative sequence (until 1%), not only zero sequence; c) misalignment of quadrature position (until 1% of relative position) from wires inside the cable. These ranges of error have been defined as the values of the individual source able to lead the output outside acceptable limits.

## 3. Results

All combinations created a setup of more than 1 million different possible scenarios. After exhaustive simulations, the error $e_{Nk}$ remains under 1p.u. in 99.9% of all scenarios, and thus compliant with adopted standards.

The maximum differential voltage on the presented results was 45.8 mV (with the 4x1.5mm$^2$ cable) and 134.9mV (with the 4x120mm$^2$ cable). Therefore, the gain A shown in amplifier of Figure 3 must be variable, in order to guarantee good dynamic range. The variation must be at least from *A=12* to *A=17* to achieve the full-scale of 3.3V on typical ADC/microprocessor system.

## 4. Conclusion

This study, proposed an assessment on contactless device for voltage harmonics measurements on low voltage multi-conductor cable. The device and the methodology are presented for four-wire cable. The theory presented here can be apply for three, two or even single wire cable with minimal adjusts. All equations were presented in continuous domain, but it can be easily mapped to discrete domain without loss of generality.

It is interesting to highlight, that connecting the reference *gnd* to the electric power system ground, instead to the *neutral*, the voltages on wires becomes: $v_{ae}$, $v_{be}$, $v_{ce}$ and $v_{ne}$, then this is a way to determine the voltage of *neutral* referred to the "earth", also with minimal adjustments.

The voltages on each individual wire can be recovered by using many capacitor plates built in the sensor around a circumference concatenating the cable, and a pilot signal, with zero sequence provided for a three-phase active calibration load. The pilot signal can be avoided if there are triples harmonics with only zero sequence on the system.

## References


1. S. Kang, S. Yang, H. Kim, Non-intrusive voltage measurement of ac power lines for smart grid system based on electric field energy harvesting, 2017, Electronics Letters, vol. 53, no. 3, pp. 181-183.
2. K.M. Tsang, W.L. Chan, Dual capacitive sensors for non-contact AC voltage measurement, 2011, Sensors Actuators, A Phys., vol. 167, no. 2, pp. 261-266.
3. D. Lawrence, J.S. Donnal, S. Leeb, Current and voltage reconstruction from non-contact field measurements, 2016, IEEE Sens. J., vol. 16, no. 15, pp. 6095–6103.
4. D. Lawrence, Hardware and Software Architecture for Non-Contact, Non-Intrusive Load Monitoring, 2016, no. 2014, Ph.D. dissertation. Department of Electrical Engineering and Computer Science. Massachusetts Institute of Technology. Massachusetts.
5. D. Lawrence, J.S. Donnal, S. Leeb, Y. He, Non-Contact Measurement of Line Voltage, 2016, IEEE Sensors Journal, vol. 16, no. 24, pp. 8990-8997.

6. D. Balsamo, D. Porcarelli, L. Benini, B. Davide, A new non-invasive voltage measurement method for wireless analysis of electrical parameters and power quality, 2013, Proc. IEEE Sensors, pp. 1–4.
7. D. Balsamo, G. Gallo, D. Brunelli, L. Benini, Non-intrusive Zigbee power meter for load monitoring in smart buildings, 2015, 2015 IEEE Sensors Appl. Symp., pp. 1–6.
8. C. Villani, S. Benatti, D. Brunelli and L. Benini, A contactless three-phase autonomous power meter, 2016, 2016 IEEE SENSORS, Orlando, FL, pp. 1-3.
9. Q. Zhou, W. He, D. Xiao, S. Li, K. Zhou, Study and experiment on non-contact voltage sensor suitable for three-phase transmission line, 2016, Sensors (Switzerland), vol. 16, no. 1, pp. 1–21.
10. S. Wei, L. Zhang, W. Gao, and Z. Cao, Non-contact voltage measurement based on electric-field effect, 2011, Procedia Eng., vol. 15, pp. 1973–1977.
11. P.S. Shenil, R. Arjun, B. George, Feasibility study of a non-contact AC voltage measurement system, 2015, Conf. Rec. - IEEE Instrum. Meas. Technol. Conf., vol. 2015, pp. 399–404.
12. K. Nakano, non-contact voltage measurement method and device, and detection probe, 2002, U.S. Patent US 2002/0167303 A1.
13. N. Nobunaga et al., Isolated voltage sensing using micro-resonator, 2013, 2013 Transducers Eurosensors XXVII 17th Int. Conf. Solid-State Sensors, Actuators Microsystems, TRANSDUCERS EUROSENSORS 2013, vol. 3, no. June, pp. 1360–1363.
14. G. McKenzie and P. Record, Non-contact voltage measurement using electronically varying capacitance, 2010, Electron. Lett., vol. 46, no. 3, p. 214.
15. Chunrong Peng, Pengfei Yang, Xiaolong Wen, Dongming Fang, and Shanhong Xia, 2014, Design of a novel micromachined non-contact resonant voltage sensor for power distribution systems, IEEE Sensors 2014. Proc., pp. 3–6.
16. C. Binkowski and C. D. Paredes Crovato, Increasing sensitivity on non-contact voltage sensor using time-varying components: A numerical analysis for accuracy assessment, 2015, 2015 IEEE Int. Work. Appl. Meas. Power Syst. AMPS 2015 - Proc.
17. G. Mckenzie and P. Record, Non-contact measurement of dc voltages using nonlinear elements G McKenzie and P Record.
18. K. Zhu, W.K. Lee, P.W.T. Pong, Non-Contact Capacitive-Coupling-Based and Magnetic-Field-Sensing-Assisted Technique for Monitoring Voltage of Overhead Power Transmission Lines, 2017, IEEE Sensors Journal, vol. 17, no. 4, pp. 1069-1083.

19. R. Hou, M. Spirito, F. Van Rijs, and L. C. N. de Vreede, Contactless Measurement of Absolute Voltage Waveforms by a Passive Electric-Field Probe, 2016, IEEE Microw. Wirel. Components Lett., vol. 26, no. 12, pp. 1008–1010.
20. M. A. Noras, Non-contact surface charge / voltage measurements Capacitive probe - principle of operation, 2002, Current, no. 3001, pp. 1–8.
21. IEC 61000-4-30 – International Standard – Electromagnetic compatibility (EMC) – Part 4-30: Testing and measurement techniques – Power quality measurement methods. (ed2 2008).
22. IEC 61000-4-7 – International Standard – Electromagnetic compatibility (EMC) – Part 4-7: Testing and measurement techniques – General guide on harmonics and interharmonics measurements and instrumentation, for power supply systems and equipment connected.
23. IEC 61000-2- 4 – International Standard – Electromagnetic compatibility (EMC) – Part 2-4: Environment - Compatibility levels in industrial plants for low-frequency conducted disturbances (ed2 2006).